Toward Unification of General Circulation and Cloud-Resolving Models

Akio Arakawa[1], Joon-Hee Jung[2] and Chien-Ming Wu[1]

[1]*University of California, Los Angeles*
California, USA
aar@atmos.ucla.edu, mog@atmos.ucla.edu

[2]*Colorado State University, Fort Collins*
Colorado, USA
jung@atmos.colostate.edu

ABSTRACT

As far as representation of deep moist convection is concerned, only two kinds of model physics are used at present: highly parameterized as in the conventional general circulation models (GCMs) and explicitly simulated as in the cloud-resolving models (CRMs). Ideally, these two kinds of model physics should be unified so that a continuous transition of model physics from one kind to the other takes place as the resolution changes. ROUTE I for the unification continues to follow the parameterization approach, but uses a unified parameterization that is applicable to any horizontal resolutions between those typically used by GCMs and CRMs. A preliminary design and partial evaluation of the unified parameterization is presented. ROUTE II for the unification follows the "multi-scale modeling framework (MMF)" approach, which takes advantage of explicit representation of deep moist convection by CRMs. The Quasi-3D (Q3D) MMF is an attempt to broaden the applicability of MMF without necessarily using a fully three-dimensional CRM. This is accomplished using a network of cloud-resolving grids with large gaps. An outline of the Q3D algorithm and highlights of preliminary results are presented.

1. Introduction

The rationale for the main theme of this paper is our recognition that the progress of our ability to represent cloud processes in climate models has been unacceptably slow (Randal *et al*. 2003). In particular, as far as representation of deep moist convection is concerned, only two kinds of model physics are used at present: *highly parameterized* and *explicitly simulated*. Correspondingly, besides those models that explicitly simulate turbulence such as Direct Numerical Simulation (DNS) and Large Eddy Simulation (LES) models, we use two discrete families of atmospheric models as shown in Fig.1: one is represented by the conventional general circulation models (GCMs) and the other by the cloud-resolving models (CRMs). In this figure, the abscissa is the horizontal resolution and the ordinate is a measure for the degree of parameterization, such as the reduction in the degrees of freedom, increasing downwards. These two families of models have been developed with applications to quite different ranges of horizontal resolution in mind.

Naturally, there have been a number of studies examining a broader applicability of each family as shown by the horizontal arrows in Fig. 1: applicability of CRMs to lower resolutions and that of GCMs to higher resolutions. Weisman *et al.* (1997), for example, examined the applicability of a CRM to squall-line simulations for midlatitude-type environments with resolutions between 1 and 12 km, and concluded that with resolutions coarser than 4 km, the evolution is characteristically slower and the resultant mature mesoscale circulation is stronger.

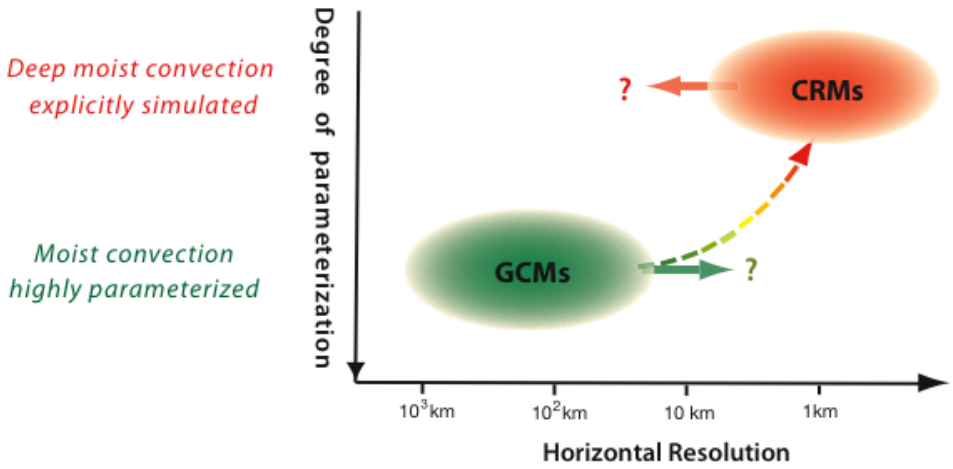

Figure 1: Two families of atmospheric models with different model physics

With respect to the applicability of GCMs to high resolutions, the work of Williamson (1999) is particularly intriguing. The paper shows that, when the horizontal resolution of the NCAR CCM2 is increased for both the dynamics and physical parameterizations, the upward branch of the Hadley circulations increases in strength and there is no sign of convergence. When the horizontal resolution is increased for the dynamics but not for the parameterizations, the solution converges. But the converged state is similar to that obtained with the coarse resolution for both so that the increased resolution for the dynamics is wasted. Together with other evidence, he concludes, "*the results raise a serious question – are the parameterizations correctly formulated in the model? . . . The parameterizations should explicitly take into account the scale of the grid on which it is based.*" A similar question on parameterization was raised by Skamarock and Klemp (1993) in the context of adaptive grid refinement. Also, analyzing the impact of horizontal resolution increases on the error growth of ECMWF forecasts, Buizza (2010) suggested that rather than resolution, it is model improvements that might lead to better predictions and longer predictability limits.

Strictly speaking, truncation of a continuous system can be justified only when the resulting error can be made arbitrarily small by using a higher resolution. Our problem is, therefore, more demanding than just a convergence; the GCM should converge to a physically meaningful high-resolution model such as a CRM applied to the global atmosphere. This requires that both the dynamics and physics of GCMs converge to those of the CRM as shown schematically by the dashed curve in Fig. 1. If the GCM and CRM share the same dynamics core, which must necessarily be nonhydrostatic, we expect that the convergence is not an issue as far as the model dynamics is concerned. Unfortunately, the same is not true for the conventional formulations of model physics, especially when cloud processes are involved.

Figure 2 schematically illustrates the qualitative difference of model physics between the two families of models. For a given observed large-scale condition, we can identify the *apparent heat source*, Q_1, and the *apparent moisture sink*, Q_2, from the residuals in large-scale heat and moisture budgets (e.g., Yanai *et al.* 1973). Here the heat source and moisture sink refer to the source of the sensible heat, $c_p T$, and the sink of the latent heat, Lq, respectively. The left panel of Fig. 2 schematically shows typical profiles of Q_1, Q_2 and $Q_1 - Q_2$ for disturbed tropical conditions. The difference $Q_1 - Q_2$ gives

the *apparent moist static energy source*. Here the moist static energy is defined by $c_pT + Lq + gz$, where gz is the geopotential energy. As we can see in the figure, the profile of $Q_1 - Q_2$ typically has negative values in the lower troposphere and positive values in the middle to upper troposphere, suggesting the dominant role of vertical eddy transport of moist static energy. Since GCMs must produce this type of profiles when deep moist convection is dominant, we call this type the "GCM-type".

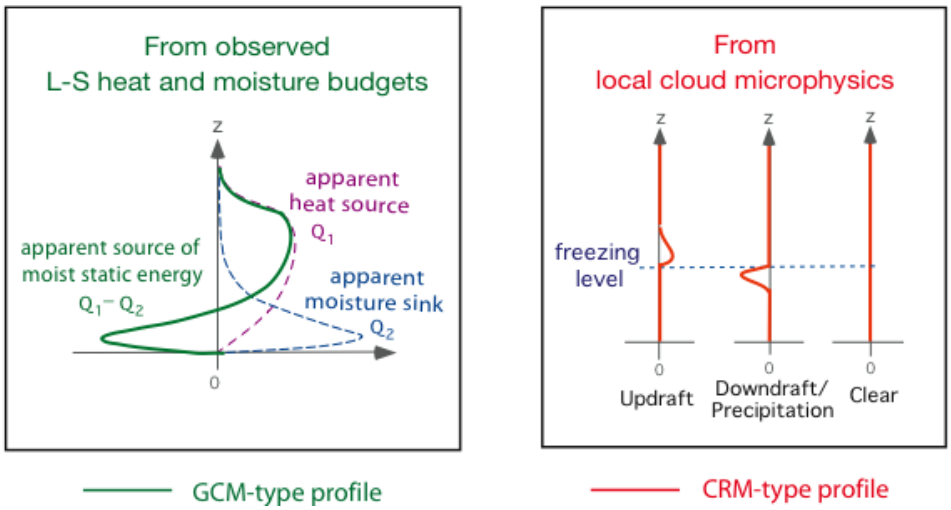

Figure 2: Schematic illustration of typical vertical profiles of moist static energy source under disturbed tropical conditions.

In contrast, the local cloud microphysical processes produce practically no moist static energy source/sink except near the freezing level. This is because moist static energy is conserved under moist-adiabatic processes and thus there is no significant source/sink of moist static energy above the surface except where the ice phase is involved. Within updrafts and downdrafts/precipitation, there are sources immediately above the freezing level due to freezing and sinks immediately below that level due to melting, respectively. These are illustrated in the right panel of Fig. 2. Cloud microphysics in CRMs is expected to produce this type of profiles, which we call the "CRM-type".

As Arakawa (2004) emphasized, it is important to recognize that any space/time/ensemble average of the CRM-type profiles does not give a GCM-type profile. This means that the cumulus parameterization problem is more than a statistical theory of cloud microphysics. Also, it is not a purely physical/dynamical problem because it is needed as a consequence of mathematical truncation. Finally, it is not a purely mathematical problem since the use of a higher resolution or an improved numerical method does not automatically improve the result. A complete theory for cumulus parameterization must address all of these aspects in a consistent manner including the transition between the GCM-type and CRM-type profiles.

We can think of two routes to achieve the unification of the two families of models. ROUTE I continues to follow the parameterization approach, but uses a unified parameterization with which the GCM converges to a global CRM (GCRM) as the grid size is refined. ROUTE II, on the other hand, replaces the parameterization of deep moist convection with a partial simulation of cloud-scale

processes by CRMs and formulates the coupling of GCM and CRMs in such a way that the coupled system converges to a GCRM as the GCM grid size is refined.

The rest of this paper is organized as follows: Section 2 discusses ROUTE I, which follows the unified parameterization approach, while section 3 discusses ROUTE II, which follows the coupled GCM/CRM approach. Finally, section 4 presents summary and further discussions.

2. ROUTE I: the unified parameterization

2.1. Identification of the problem

The starting point of Route I is the fact that most of the existing cumulus parameterization schemes including Arakawa an Schubert (1974) assume $\sigma << 1$, either explicitly or implicitly, where σ is the fractional area covered by all convective clouds in the grid cell. With this assumption, the temperature and water vapor to be predicted are essentially those for the cloud environment. Then, as illustrated by the red arrows in Fig. 3(a), relevant physical processes are the "cumulus-induced" subsidence in the environment and the detrainment of cloud air into the environment. [Here it is important to note that the "cumulus-induced subsidence" is a hypothetical subsidence. The true subsidence is the sum of the blue and red arrows in Fig. 3(a), which tend to compensate each other under normal circumstances. In such a case, the true subsidence occurs in another grid cell, which may well be far away, whose position is determined by the grid-scale dynamics, not by the parameterization.]

As the grid size becomes smaller, however, the cloud may eventually occupy the entire grid cell so that there is no "environment" within the same grid cell. Then, as Fig. 3(b) indicates, the probability density function of σ becomes bimodal in this limit, consisting of $\sigma = 1$ and $\sigma = 0$ (Krueger 2002, Krueger and Luo 2004). It is then clear that a key to open ROUTE I is to include a transition to this limit by eliminating the assumption of $\sigma << 1$.

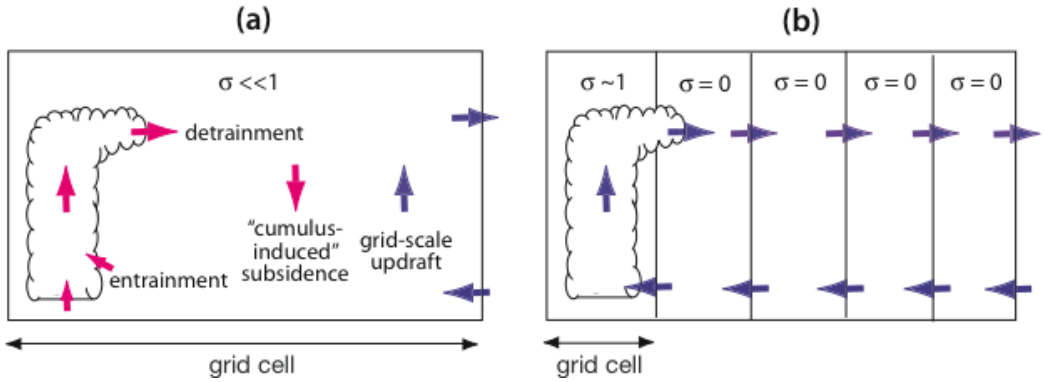

Figure 3: Schematic illustration of circulations associated with clouds for (a) coarse and (b) fine resolutions.

To visualize the problem raised above, we have analyzed datasets simulated by a CRM as Krueger (2002) and Krueger and Luo (2004) did. The simulations we used are performed by applying the 3D anelastic vorticity equation model of Jung and Arakawa (2008) to a horizontal domain of 512 km × 512 km with a 2 km horizontal grid size. Other experimental settings are similar to the benchmark

simulations used by Jung and Arakawa (2010). Two 24-hour simulations are made, one with and the other without background shear. Figure 4 shows snapshots of vertical velocity *w* at 3km height at the end of these simulations. As is clear from these snapshots, the two simulations represent quite different cloud regimes. For the analysis presented in this paper, datasets are taken from the last 2-hour period of each simulation with 20-min intervals.

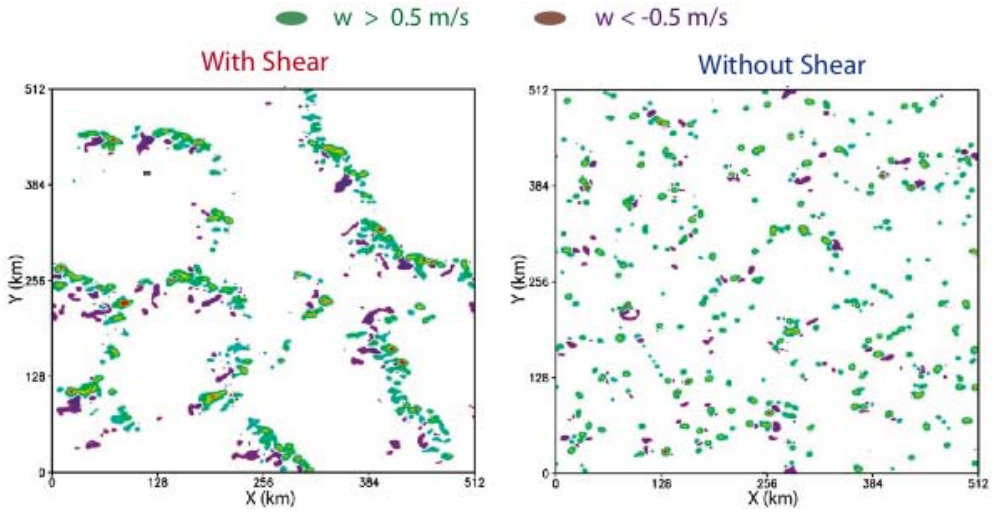

Figure 4: Snapshots of vertical velocity w *at 3 km height at the end of two simulations with and without background shear.*

To analyze the resolution dependency of the statistics of data, we divide the original 512 km domain into sub-domains of equal size. The selected side lengths of the sub-domains are $d_n = 512\,\mathrm{km}/2^{n-1}$, $n = 2,3,4,\ldots,9$. The original domain can then be identified by $n = 1$. Figure 5 shows the original and examples of the sub-domains. In the analysis presented here, grid points that satisfy *w* > 0.5 m/s are considered as "cloud points".

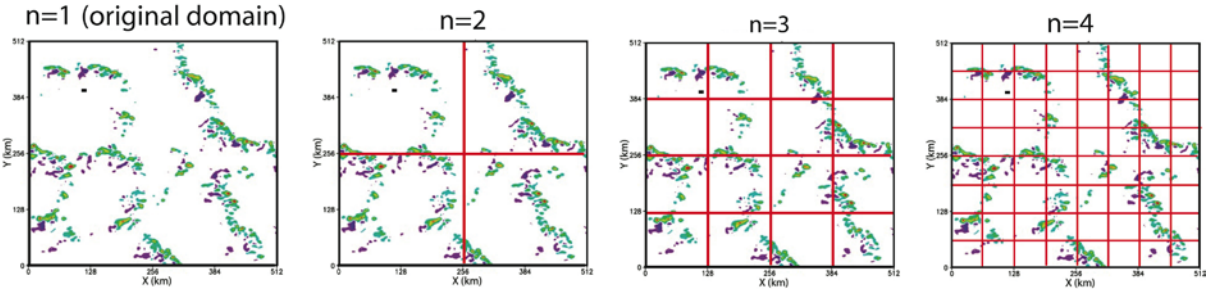

Figure 5: The original domain and examples of the sub-domains used for analysis.

Figure 6 shows σ at 3km height averaged over all cloud-containing (i.e., $\sigma \neq 0$) sub-domains and its standard deviation against the sub-domain sizes d_n for the shear case (a) and non-shear case (b). It is clear that for both cases, $\sigma << 1$ can be a good approximation only for coarse resolutions, say, $d_n \geq 32$ km, and σ tends to increase as d_n decreases and becomes 1 for d_n = 2 km, which is the grid size used by the CRM. The standard deviation is very large for high resolutions, but it is expected since there is no reason to believe that σ is a unique function of d_n. In spite of the large standard deviation,

however, the tendency toward a bimodal distribution consisting of $\sigma = 1$ and $\sigma = 0$ can be seen for high resolutions. We see that σ tends to be larger for the shear case than the non-shear case. The number of cloud-containing sub-domains is, however, smaller for the shear case (not shown).

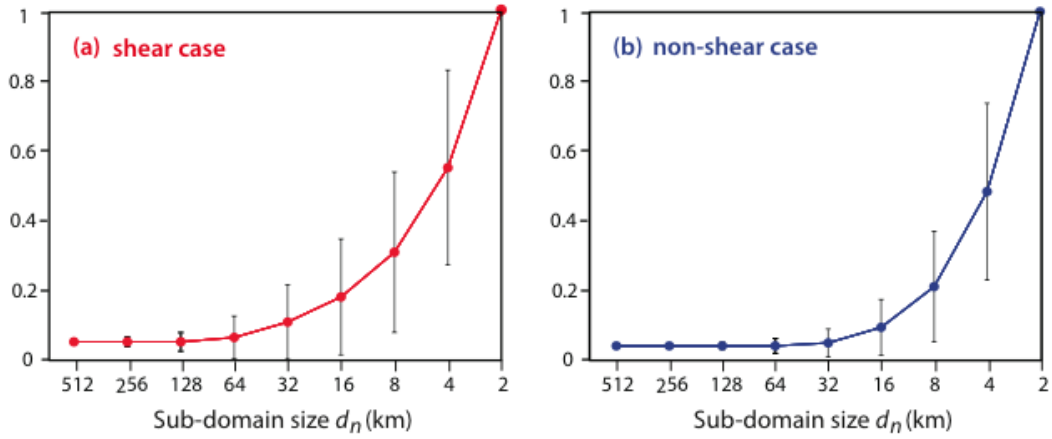

Figure 6: Dependence of the mean fractional cloud cover at 3 km height on the sub-domain size and its standard deviation.

2.2. Expressions for vertical eddy transport

Recall that the vertical eddy transport of moist static energy is responsible for the difference between the GCM-type and CRM-type profiles illustrated with Fig. 2. We now attempt to formulate the vertical eddy transport of thermodynamic variables in a way that is applicable to any values of σ including 1. In this paper, we consider the vertical eddy transport of water vapor mixing ratio, q, as an example. As is commonly done in conventional cumulus parameterization schemes, we assume that the cloud and environment values of q, denoted by q_c and $\tilde{q}$, respectively, are horizontally uniform individually. The existence of convective-scale downdrafts is ignored at this stage.

Let an overbar denote the mean over the entire area of grid cell. Then,

$$\overline{q} = \sigma q_c + (1-\sigma)\tilde{q}\,. \tag{1}$$

Further let w_c and $\tilde{w}$ be the averages of w over the clouds and the environment, respectively. Then,

$$\overline{w} = \sigma\, w_c + (1-\sigma)\tilde{w} \tag{2}$$

and

$$\overline{wq} = \sigma\, w_c\, q_c + (1-\sigma)\tilde{w}\tilde{q}\,. \tag{3}$$

from (3) with (1) and (2), we find

$$\overline{wq} - \overline{w}\,\overline{q} = \sigma(1-\sigma)\left(w_c - \tilde{w}\right)\left(q_c - \tilde{q}\right). \tag{4}$$

The left hand side of (4) is the vertical eddy transport of q per unit horizontal area and density, which we simply call the "eddy transport" of q. As expected, the eddy transport vanishes for $\sigma = 0$ and $\sigma = 1$. The expression (4) is, however, not convenient to use due to the appearance of the environment values, $\tilde{w}$ and $\tilde{q}$, which are not well defined for situations $\sigma \sim 1$. We thus eliminate these variables using (1) and (2). After some manipulations, we find

$$\overline{wq} - \overline{w}\,\overline{q} = \frac{\sigma}{1-\sigma}\left(w_c - \overline{w}\right)\left(q_c - \overline{q}\right). \tag{5}$$

2.3. Requirement for convergence

We now introduce the requirement that the parameterization converge to explicit simulations of cloud processes as $\sigma \to 1$ and thus

$$\lim_{\sigma\to 1} w_c = \overline{w} \quad \text{and} \quad \lim_{\sigma\to 1} q_c = \overline{q}\,. \tag{6}$$

This means that both $w_c - \overline{w}$ and $q_c - \overline{q}$ are the order of $1-\sigma$ (or higher) so that $\left(w_c - \overline{w}\right)\left(q_c - \overline{q}\right)$ is the order of $(1-\sigma)^2$ (or higher) near this limit. The simplest choice to satisfy this requirement is

$$\left(w_c - \overline{w}\right)\left(q_c - \overline{q}\right) = (1-\sigma)^2\left(w_c^* - \overline{w}\right)\left(q_c^* - \overline{q}\right), \tag{7}$$

where an asterisk represents a value expected when $\sigma << 1$. Substituting (7) into (5), we obtain

$$\overline{wq} - \overline{w}\,\overline{q} = \sigma(1-\sigma)\left(w_c^* - \overline{w}\right)\left(q_c^* - \overline{q}\right)\,. \tag{8}$$

Equation (8) represents the basic structure of the unified parameterization.

For the convenience in practical applications, we rewrite (5) as follows. Using w_c^* and q_c^* for w_c and q_c in (5), respectively, the vertical eddy transport expected when $\sigma << 1$ is given by

$$\left(\overline{wq} - \overline{w}\,\overline{q}\right)^* = \frac{\sigma}{1-\sigma}\left(w_c^* - \overline{w}\right)\left(q_c^* - \overline{q}\right). \tag{9}$$

Then (8) may be rewritten as

$$\overline{wq} - \overline{w}\,\overline{q} = (1-\sigma)^2\left(\overline{wq} - \overline{w}\,\overline{q}\right)^*. \tag{10}$$

When σ is finite, (10) shows that the actual eddy transport is less than $\left(\overline{wq} - \overline{w}\,\overline{q}\right)^*$ due to the factor $(1-\sigma)^2$, giving $\overline{wq} - \overline{w}\,\overline{q} = 0$ for $\sigma = 1$. To complete the design of the unified parameterization, we must decide on ways to determine σ and $\left(\overline{wq} - \overline{w}\,\overline{q}\right)^*$.

2.4. A partial evaluation of the unified parameterization

Before proceeding to the design of algorithms to determine σ and $\left(\overline{wq}-\overline{w}\,\overline{q}\right)^*$, we present a partial evaluation of the unified parameterization again using the dataset mentioned in subsection 2.1. The evaluation is designed to examine the validity of the formal structure of the parameterization in a way independent of the errors from particular choices of the algorithms to determine σ and $\left(\overline{wq}-\overline{w}\,\overline{q}\right)^*$.

Let X be a variable defined for each sub-domain. For a compact presentation of the results, we define a *weighted ensemble average* $\langle X \rangle$ by the average of σX over all sub-domains divided by the average of σ itself. We use the weight σ to reduce or eliminate the contribution from sub-domains that have few or no clouds. The weighted ensemble averages of (5), (7) and $\sigma/(1-\sigma)\times$(7) are

$$\left\langle \overline{wq}-\overline{w}\,\overline{q} \right\rangle = \left\langle \frac{\sigma}{1-\sigma}\left(w_c-\overline{w}\right)\left(q_c-\overline{q}\right) \right\rangle, \tag{11}$$

$$\left\langle \left(w_c-\overline{w}\right)\left(q_c-\overline{q}\right) \right\rangle = \left\langle \left(1-\sigma\right)^2 \right\rangle \left(w_c^*-\overline{w}\right)\left(q_c^*-\overline{q}\right) \tag{12}$$

and

$$\left\langle \frac{\sigma}{1-\sigma}\left(w_c-\overline{w}\right)\left(q_c-\overline{q}\right) \right\rangle = \left\langle \sigma\left(1-\sigma\right) \right\rangle \left(w_c^*-\overline{w}\right)\left(q_c^*-\overline{q}\right), \tag{13}$$

respectively. In deriving (12) and (13), we have ignored the difference of $\left(w_c^*-\overline{w}\right)\left(q_c^*-\overline{q}\right)$ between the sub-domains because it represents a hypothetical property of clouds (relative to the mean field) for the situation $\sigma << 1$. Eliminating $\left(w_c^*-\overline{w}\right)\left(q_c^*-\overline{q}\right)$ between (12) and (13) and using the result in (11), we obtain

$$\left\langle \overline{wq}-\overline{w}\,\overline{q} \right\rangle = \frac{\left\langle \sigma\left(1-\sigma\right) \right\rangle}{\left\langle \left(1-\sigma\right)^2 \right\rangle} \left\langle \left(w_c-\overline{w}\right)\left(q_c-\overline{q}\right) \right\rangle. \tag{14}$$

The partial evaluation presented here specifically examines the validity of the relation (14) using the values diagnosed from the dataset. The right hand side of (14) depends on the resolution through the two factors, $\left\langle \sigma\left(1-\sigma\right) \right\rangle \Big/ \left\langle \left(1-\sigma\right)^2 \right\rangle$ and $\left\langle \left(w_c-\overline{w}\right)\left(q_c-\overline{q}\right) \right\rangle$. The open triangles in Fig. 7 show the dependency through the latter by replacing σ in the former with prescribed constant values, 0.1~0.5. Not surprisingly, this quantity strongly depends on the value of σ. For coarse resolutions with small values of σ, it is rather insensitive to the sub-domain size d_n, but it rapidly decreases from the medium to high resolutions as w_c and q_c become closer to $\overline{w}$ and $\overline{q}$. As expected, it eventually vanishes when d_n becomes 2 km, which is the grid size of the CRM used. It is interesting to see that the non-shear case transports water vapor more efficiently than the shear case.

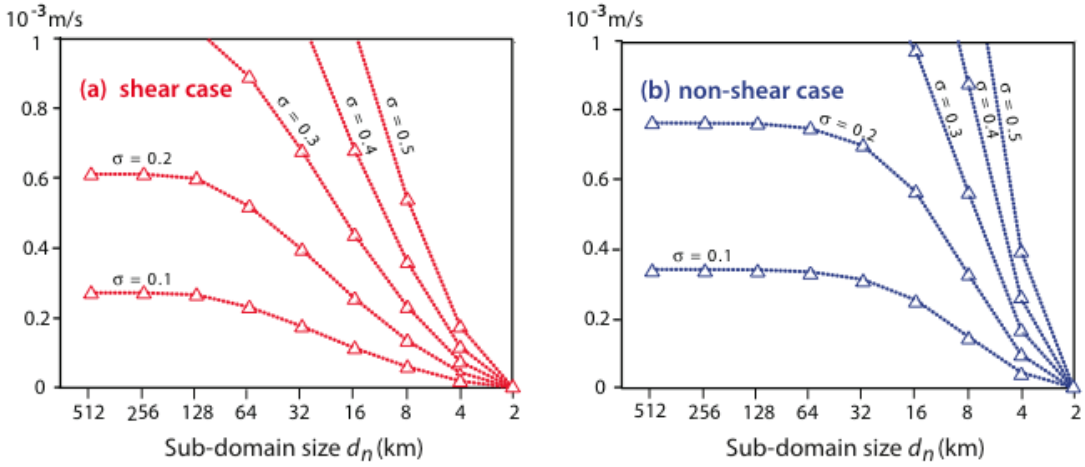

Figure 7: Weighted ensemble average of the eddy transport of water vapor at 3 km height estimated with the right hand side of (14) using a prescribed constant σ.

The open circles in Fig. 8 show the values of $\left\langle \overline{wq} - \overline{w}\,\overline{q} \right\rangle$ at 3 km height estimated with the right hand side of (14) using σ diagnosed from the dataset. Drastic differences of the resolution dependence from those shown in Fig. 8 are apparent. The qualitative differences for coarse resolutions are due to the small values of σ. For verification, the values of $\left\langle \overline{wq} - \overline{w}\,\overline{q} \right\rangle$ directly calculated from the dataset without using the assumptions behind (5) and (7) are shown by the solid circles. Amazingly, the resolution dependence of the estimated values is very similar to that of the directly calculated values. The magnitude of the estimated values are, however, systematically smaller than that of the directly calculated values. This is not surprising in view of the various idealizations used, such as neglecting convective downdrafts and possible coexistence of different types of clouds and different phases of cloud development. In any case, the results presented here underscore the importance of including the effect of variable σ in cumulus parameterization.

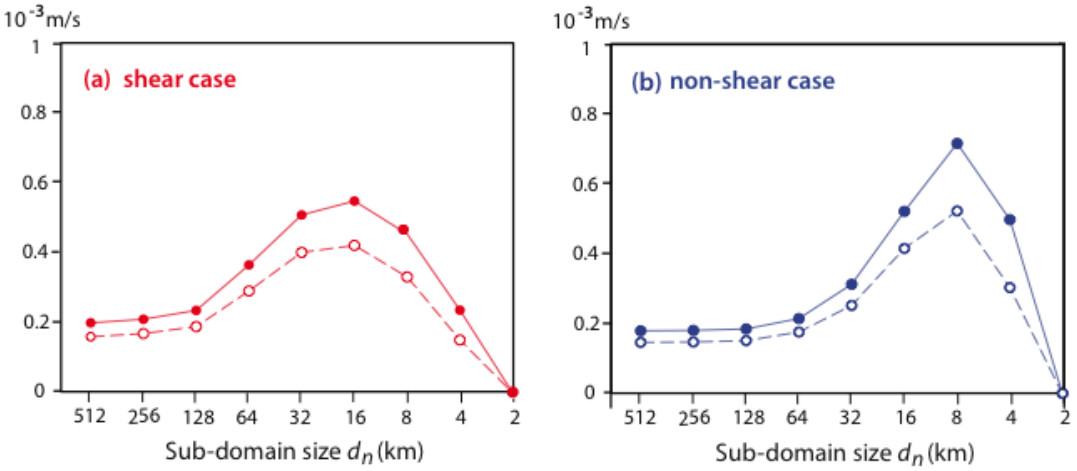

Figure 8: Weighted ensemble average of the eddy transport of water vapor at 3 km height. Open circles: estimated with the right hand side of (14) using diagnosed σ. Closed circles: Diagnosed from data using the left hand side of (14).

2.5. Determination of σ

The closure of conventional cumulus parameterization schemes determines the apparent source of thermodynamic prognostic variables. For q, for example, it is given by $S_q - \partial\rho\left(\overline{wq} - \overline{w}\,\overline{q}\right) / \rho\partial z$, where S_q is the true source of q per unit mass due to sub-grid cloud processes and ρ is the density. From this together with S_q determined by the parameterization, the eddy transport $\overline{wq} - \overline{w}\,\overline{q}$ can be calculated. Let the value of $\overline{wq} - \overline{w}\,\overline{q}$ determined in this way be $\left(\overline{wq} - \overline{w}\,\overline{q}\right)_{\text{adj}}$. Here the suffix adj is used because most of the conventional schemes can be interpreted as adjustment schemes (Arakawa 2004). We then assume that $\left(\overline{wq} - \overline{w}\,\overline{q}\right)_{\text{adj}}$ can be used for $\left(\overline{wq} - \overline{w}\,\overline{q}\right)^*$ in (9) so that σ is given by

$$\sigma = \frac{\left(\overline{wq} - \overline{w}\,\overline{q}\right)_{\text{adj}}}{\left(\overline{wq} - \overline{w}\,\overline{q}\right)_{\text{adj}} + \left(w_c^* - \overline{w}\right)\left(q_c^* - \overline{q}\right)}. \qquad (15)$$

The unified parameterization uses σ determined in this way. We see that the condition $0 \le \sigma \le 1$ is automatically satisfied by (15), as long as $\left(\overline{wq} - \overline{w}\,\overline{q}\right)_{\text{adj}}$ and $\left(w_c^* - \overline{w}\right)\left(q_c^* - \overline{q}\right)$ have the same sign, with $\sigma \to 0$ as $\left(\overline{wq} - \overline{w}\,\overline{q}\right)_{\text{adj}} \to 0$ and $\sigma \to 1$ as $\left(\overline{wq} - \overline{w}\,\overline{q}\right)_{\text{adj}} \to \infty$.

As far as the basic reasoning is concerned, the above approach to determine σ is in parallel to Emanuel (1991) in the sense that the following two information are combined: vertical profiles of cloud properties determined by a cloud model and the total vertical transport necessary to maintain a quasi-equilibrium.

2.6. Anticipated impact of the unified parameterization and remaining problems

In this section, we have presented a new framework for cumulus parameterization in which the result of parameterization converges to an explicit simulation of cloud processes as the resolution increases. Thus the new parameterization unifies parameterizations in GCMs and those in CRMs as far as representation of deep moist convection is concerned. With the unified parameterization, the error of the GCM solution in satisfying the CRM equations can be made arbitrarily small by using a higher resolution. In this way, multi-scale numerical methods such as multiply-nested grids and adaptive mesh refinement (AMR) methods, for example, can be used with no problem in model physics. We emphasize that this drastic broadening of the applicability of cumulus parameterization can be achieved by a relatively minor modification of the conventional mass-flux based parameterization schemes. However, a good cloud model to determine $\left(w_c^* - \overline{w}\right)\left(q_c^* - \overline{q}\right)$ and a reasonable closure applicable to coarse resolutions to determine the magnitude of $\left(\overline{wq} - \overline{w}\,\overline{q}\right)_{\text{adj}}$ are prerequisites to the success of the unified parameterization. Also, the dynamics and formulations of cloud microphysics, turbulence and radiation must be such that they are applicable to a wide range of resolutions.

There are two main sources for uncertainty in the results of the unified parameterization: one is the non-deterministic nature of the closure, as discussed by Xu and Arakawa (1992), and the other is estimating cloud properties with huge dimensions by a simple cloud model. This may suggest the necessity of including a stochastic component in the parameterization. We note, however, that such a component is not needed near the limit of $\sigma \to 1$ because the explicit simulation by the CRM can act as a random-process generator by itself.

When it is successfully implemented, the practical merits of the unified parameterization will be great. But we should remember that it has a limit as a "parameterization", which inevitably requires a number of idealizations to reduce the degrees of freedom. When sufficient computer resources are available, therefore, we should pursue the other approach, ROUTE II, for more realistic numerical weather prediction and climate simulations as discussed in the next section.

3. Route II: Quasi-3D Multiscale Modeling Framework

We have developed Quasi-3D Multi-scale Modeling Framework (Q3D MMF) following ROUTE II for unification of GCMs and CRMs through explicitly simulating the details of cloud processes at least partially. The Q3D MMF is described in detail by Jung and Arakawa (2010) so that this paper gives only a brief outline of the framework and some highlights of its preliminary results.

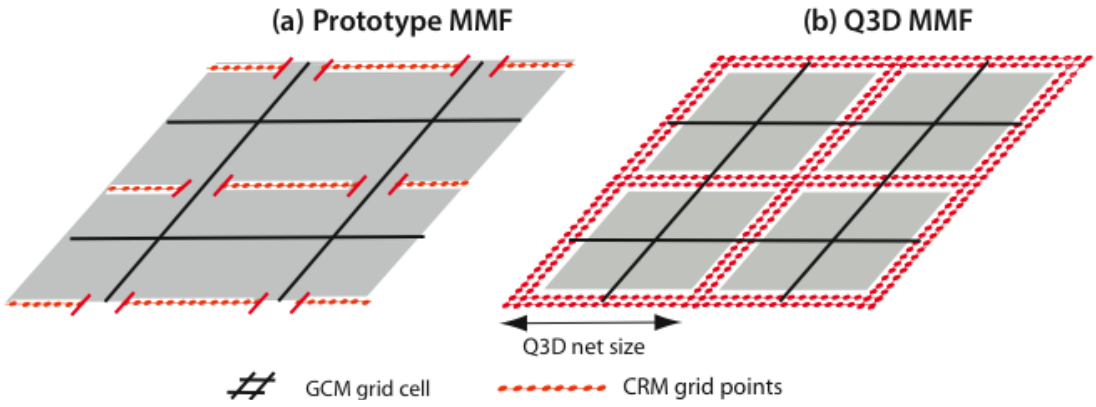

Figure 9: Examples of grid-point arrays used in the Prototype and Q3D MMFs.

MMF recognizes that we currently have two kinds of model physics, the GCM type and the CRM type. Correspondingly, MMF uses two grid systems, one for the GCM and the other for the CRM. Model physics is almost entirely determined by the statistics of CRM solutions, replacing the conventional parameterizations in GCMs. In contrast to many other multi-scale numerical methods, MMF gains computing efficiency by sacrificing full representation of cloud-scale 3D processes. This is motivated by the fact that 2D CRMs are reasonably successful in simulating thermodynamical effects of deep moist convection. The prototype MMF is called "Cloud Resolving Convective

Parameterization" (Grabowski and Smolarkiewicz 1999; Grabowski 2001) or "Super Parameterization" (Khairoutdinov and Randall 2001; Randall *et al.* 2003). It replaces the cloud parameterization by a 2D CRM embedded in each GCM grid cell as shown in Fig. 9(a) for a portion of the horizontal domain. The MMF is still called "parameterization" because it inherits the structure of conventional GCM; *i.e.*, the CRM is forced by the GCM and the GCM recognizes only the domain-averaged values of the CRM results.

The Quasi-3D (Q3D) MMF we have developed is an attempt to broaden the applicability of the prototype MMF without necessarily using a fully three-dimensional CRM. The horizontal domain of the Q3D MMF consists of a network of perpendicular sets of channels, each of which contains grid-point arrays as shown in Fig. 9(b). The grey areas in the figure represent the gaps of the network. For computing efficiency, the gaps are chosen to be large by using a narrow width for the channels, barely enough to cover a typical cloud size in the lateral direction. Thus, a channel may contain only a few grid-point arrays, whose minimum number required for resolving local 3D processes is two as in Fig. 9(b).

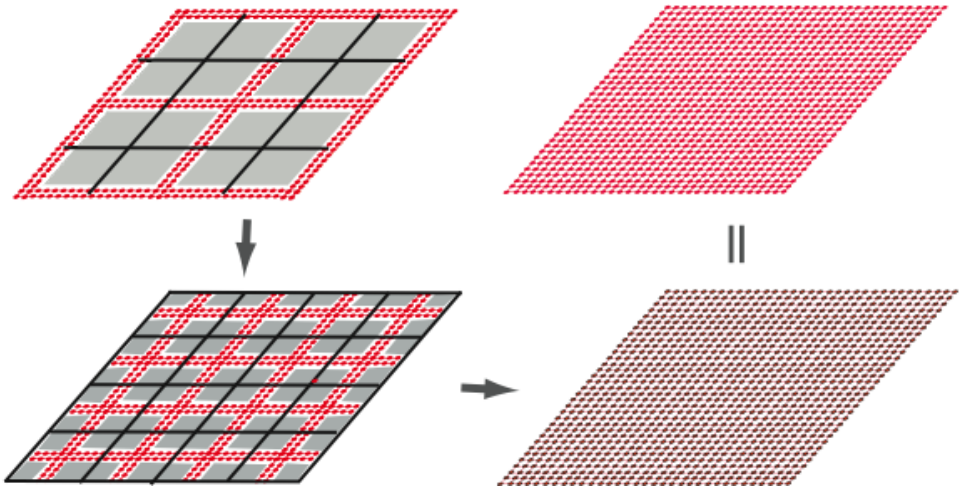

Figure 10: Schematic illustration of the convergence of the Q3D MMF grid to a 3D CRM grid.

Because the channels are so narrow, it is crucial to select a proper lateral boundary condition to realistically simulate the statistics of cloud and cloud-associated processes. Among the various possibilities, a periodic lateral boundary condition is chosen for the deviation from a background field obtained through interpolation from GCM grid points. We design the coupling of the two grid systems in such a way that the deviation vanishes as the GCM grid size approaches that of the CRM. Thus the whole system of the Q3D MMF can formally converge to a fully 3D global CRM as schematically shown in Fig. 10. Consequently, the horizontal resolution of the GCM can be freely chosen depending on the objective of application without changing the formulation of model physics. For more details of the Q3D algorithm, see Jung and Arakawa (2010).

To evaluate the Q3D CRM in an efficient way, idealized experiments are performed using a small horizontal domain. First, benchmark simulations are made using a fully 3D CRM. Then a Q3D simulation is made for the situation corresponding to each of the benchmark simulations. The grid used in these tests is similar to that in the central GCM grid cell of Fig. 9(b), consisting of only one pair of perpendicular channels with only two grid points across each channel. Since the horizontal domain is so small, the GCM component is made inactive in these tests. Thus the GCM grid point values are taken from the benchmark simulations after horizontal smoothing. These values are then interpolated to provide the background field. With the domain size and the CRM grid size used, the ratio of the number of grid points of the Q3D and 3D CRMs is only 3%. In the figures shown below, red and black lines represent the results of the Q3D and corresponding benchmark (BM) simulations, respectively, averaged over the respective horizontal domain.

Figure 11 shows time series of precipitation, evaporation and sensible heat flux at the surface. The Q3D results fluctuate more than those of the BM because the sample size of the former is much smaller than that of the latter. The time averages of the Q3D results are, however, quite close to those of the BM.

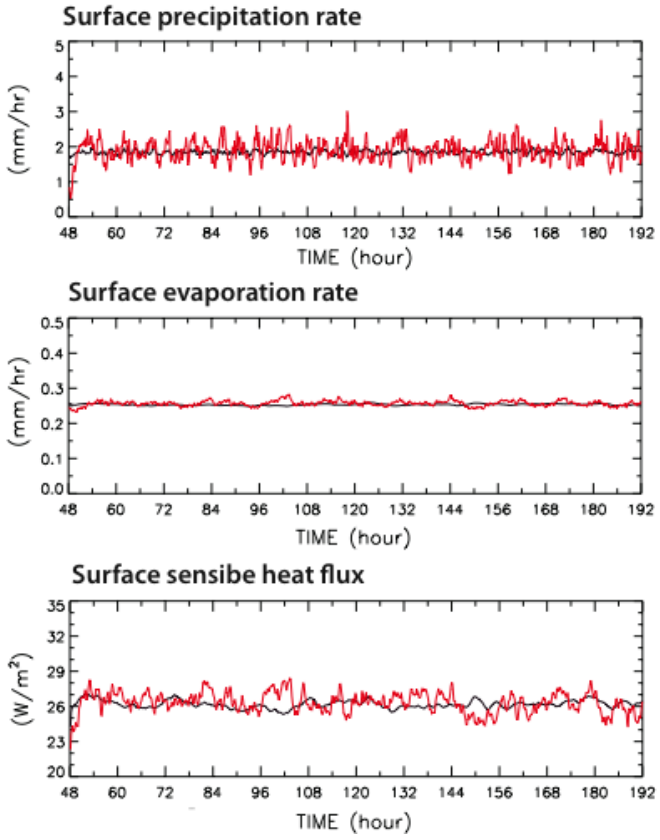

Figure 11: See text for explanation.

The upper panels of Fig. 12 show vertical profiles of the time- and domain-averaged vertical transports of potential temperature and water vapor mixing ratio. The vertical transport of potential temperature, which is a measure of the buoyancy generation of kinetic energy, is slightly under-predicted by the Q3D. On the other hand, the vertical transport of water vapor shows an almost perfect agreement with the BM. The lower panels of Fig. 12 show vertical profiles of the time- and

domain-averaged transports of the horizontal components of vorticity. The positive sign in the figure is chosen to represent the acceleration of mean flow. These figures show that the transports of vorticity components are also well simulated in the Q3D runs. This is especially encouraging because it indicates that the Q3D CRM simulates the cloud-scale 3D processes reasonably well in spite of the use of the highly limited number of grid points across the channels.

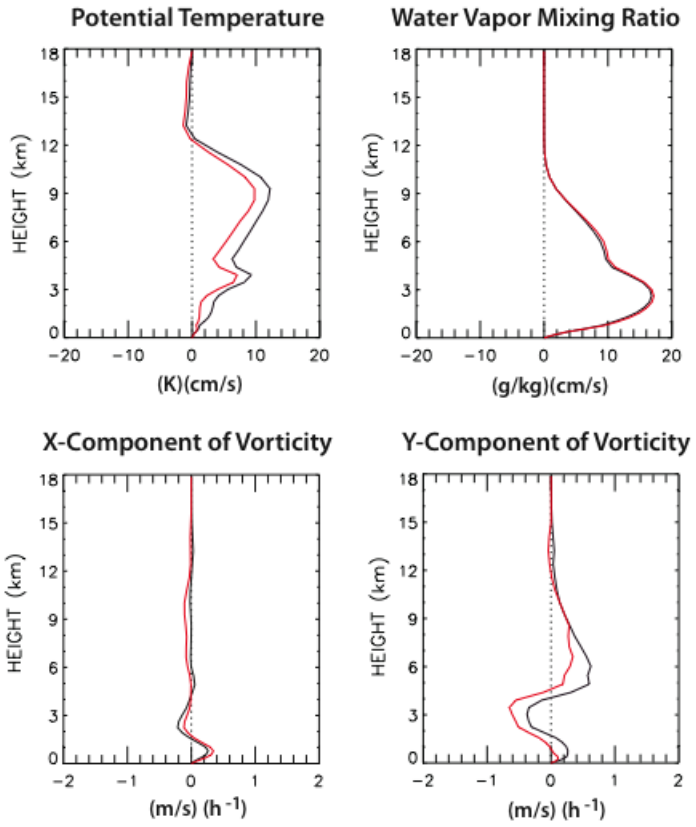

Figure 12: See text for explanation.

More details of these tests are shown in Jung and Arakawa (2010) including comparisons with 2D and coarse 3D runs. Overall, Route II with the Q3D CRM is extremely promising since its results are close to that of a 3D CRM while computationally it is more efficient by almost two orders of magnitude.

4. Summary and conclusion

As far as representation of deep moist convection is concerned, conventional GCMs and CRMs have quite different formulations of model physics, each of which is applicable to only a limited range of horizontal resolution. These two kinds of model physics should be unified so that a continuous transition from one kind to the other takes place as the resolution changes. Then a resolution between those typically used by GCMs and CRMs can be freely chosen depending on the objective of the application.

This paper suggests two possible routes to achieve the unification. ROUTE I uses a new framework for cumulus parameterization in which the result of parameterization converges to an explicit simulation of cloud processes as the resolution increases. In this way the framework unifies parameterizations in GCMs and CRMs as far as representation of deep moist convection is concerned. With the unified parameterization, the error of the GCM solution in satisfying the CRM equations can be made arbitrarily small by using a higher resolution. It is shown that a key to construct a unified parameterization is to eliminate the assumption of small fractional area covered by convective clouds, which is commonly assumed in the conventional cumulus parameterizations either explicitly or implicitly. A preliminary design of the unified parameterization is presented, which demonstrates that such an assumption could be eliminated through a relatively minor modification of the existing mass-flux based parameterizations. A partial evaluation of the unified parameterization is also presented.

When it is successfully implemented, the practical merits of the unified parameterization will be great. But it has a limit as a "parameterization", which inevitably requires a number of idealizations to reduce the degrees of freedom. When sufficient computer resources are available, therefore, we should pursue the other approach, ROUTE II, which follows the MMF approach to statistically couple GCM and CRM grids. The Quasi-3D (Q3D) MMF is an attempt to broaden the applicability of the prototype MMF without necessarily using a fully three-dimensional CRM. A great advantage of the Q3D MMF is that it converges to a 3D CRM as the GCM's resolution is refined while maintaining the same CRM physics throughout. An outline of the Q3D algorithm and highlights of preliminary results are presented. Comparing the simulation results with the corresponding benchmark simulation performed with a 3D CRM, it is concluded that the Q3D CRM can reproduce most of the important statistics of the 3D solutions, including precipitation rate and heat fluxes at the surface and vertical profiles of vertical transports of major prognostic variables.

The Q3D MMF and GCMs with the unified parameterization still represent different families of models. As shown in Fig. 13, however, the both can converge to the same model, a GCRM, as the GCM resolution approaches the CRM resolution. Comparisons of simulated results from these models with those from a GCRM will greatly enhance our understanding of the multiscale role of cumulus convection in the global atmosphere.

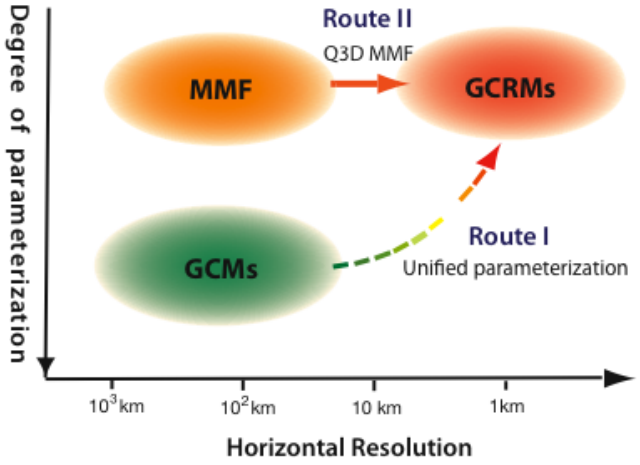

Figure 13: Two routes to unify coarse- and fine-resolution models.

Acknowledgments

We wish to thank Professor David Randall for his interest and support of this work. This research has been supported by the National Science Foundation Science and Technology Center for Multi-Scale Modeling of Atmospheric Processes, managed by Colorado State University under cooperative agreement No. ATM-0425247.

References

Arakawa, A., 2004: The cumulus parameterization problem: Past, present, and future. *J. Climate*, **17**, 2493–2525.

Arakawa, A., and W. H. Schubert, 1974: Interaction of a cumulus cloud ensemble with the large-scale environment. Part I. *J. Atmos. Sci.*, **31**, 674-701.

Buizza, R., 2010: Horizontal resolution impact on short and long-range forecast error. *Q. J. R. Meteorol. Soc.*, **136**, 1020–1035.

Emanuel, K. A., 1991: A scheme for representing cumulus convection in large-scale models. *J. Atmos. Sci.*, **48**, 2313-2335.

Grabowski, W. W., and P. K. Smolarkiewicz, 1999: CRCP: a cloud resolving convective parameterization for modeling the tropical convective atmosphere. *Phicica D*, **133**, 171–178.

Grabowski, W. W., 2001: Coupling cloud processes with the large-scale dynamics using the cloud-resolving convective parameterization (CRCP). *J. Atmos. Sci.*, **58**, 978-997.

Jung, J.-H., and A. Arakawa, 2008: A three-dimensional anelastic model based on the vorticity equation. *Mon. Wea. Rev*. **135**, 276-294.

Jung, J.-H., and A. Arakawa, 2010: Development of a quasi-3d multiscale modeling framework: motivation, basic algorithm and preliminary results. *J. Adv. Model. Earth Syst.*, **2**, Art. #11, 31 pp.

Khairoutdinov, M. F., and D. A. Randall, 2001: A cloud-resolving model as a cloud parameterization in the NCAR Community Climate System Model: Preliminary results. *Geophys. Res. Lett.*, **28**, 3617-3620.

Krueger, S. K., 2002: Current Issues in Cumulus Parameterization. *ECMWF Seminar on Key issues in the Parameterization of Subgrid Physical Processes*, ECMWF, Reading, 3–7 September 2001, 25–51.

Krueger, S. K., and Y. Luo, 2004: Grid-size dependence of cumulus parameterization. Extended Abstracts, 20th Conference on Weather Analysis and Forecasting/16th Conference on Numerical Weather Prediction, Seattle, WA, Amer. Meteor. Soc.

Randall, M. Khairoutdinov, A. Arakawa and W. Grabowski, 2003: Breaking the cloud parameterization deadlock. *Bull. Amer. Meteor. Soc.*, **84**, 1547-1564.

Skamarock, W. C. and J. B. Klemp, 1993: Adaptive grid refinement for two-dimensional and three-dimensional nonhydrostatic atmospheric flow. *Mon. Wea. Rev*, **121**, 788–804

Weisman, M. L., W. C. Skamarock, and J. B. Klemp, 1997: The resolution dependence of explicitly modeled convective system. *Mon. Wea. Rev*, **125**, 527–548.

Williamson, D. L., 1999: Convergence of atmospheric simulations with increasing horizontal resolution and fixed forcing scales. Tellus, 51A, 663–673.

Xu, K.-M., and A. Arakawa, 1992: Semi-prognostic tests of the Arakawa-Schubert cumulus parameterization using simulated data. *J. Atmos. Sci.,* **49**. 2421-2436.

Yanai, M., S. Esbensen and J. Chu, 1973: Determination of bulk properties of tropical cloud clusters from large-scale heat and moisture budgets. *J. Atmos. Sci.,* **30**, 611-627.